Towards a complexity measure theory for vortex tangles

Renzo L. Ricca

Department of Mathematics, University College London
Gower Street, London WC1E 6BT, UK
E-mail: ricca@math.ucl.ac.uk

Abstract

In this paper we address the problem of measuring structural complexity of
generic tangles of vortex lines in a fluid domain, by using a combination of geo-
metric and topological techniques. To this end new concepts based on the idea
of structural 'tropicity' are introduced to determine 'tubeness', 'sheetness' and
'bulkiness' of a vortex tangle and to evaluate the degree of topological entan-
glement. A number of cases are considered: from highly organised, coherent
vortex regions, given by the embedding of vortex coils, knots and links on
nested tori, to less organised vortical flows, such as tangles of chaotic vortex
lines. Various measures of linking (and helicity) are presented as well as esti-
mates of writhing and crossing numbers based on geometric and topological
information. Moreover, by using the concept of signature preserving flow we
extend the definition of classical stability to include wilder vortex dynamics
that during evolution preserve structural complexity. The tools and the new
concepts presented in this paper are useful for the classification and study of
general flow fields and can be employed to develop computational techniques
for measuring structural complexity.

1 Vortex structures as complex tangles of vortex lines

Modelling and control of turbulent flows still defy mathematics for difficulty and
complexity. Spontaneous formation and interaction of self-organized, coherent vor-
tex regions are generic features of turbulent flows (Vincent & Meneguzzi, 1991;
Jiménez *et al.*, 1993). Coherence (for a proper definition see §6 below) is essentially
due to the strong correlation of dynamical properties (such as fluid pressure, veloc-
ity, vorticity, strain, etc.) confined to localized regions in the fluid domain $\mathcal{D}$. These
regions are occupied by extended, filamentary 'structures' in the shape of vortex
tubes and sheets (see, for example, Schwarz, 1988; She *et al.*, 1990; figure 1). These
structures are present where vorticity $\omega(\mathbf{X}, t) = \nabla \times \mathbf{u}(\mathbf{X}, t)$ (where $\mathbf{u}(\mathbf{X}, t)$ denotes
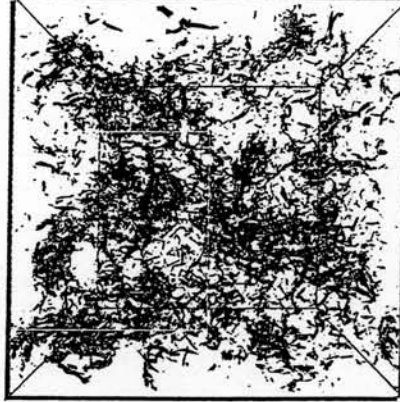
Figure 1: Localization of vortex structures in a visualization of data from 512^3-element turbulence simulation in a numerical box (from Fernandez *et al.*, 1996).

fluid velocity and everything is smooth function of the position vector $\mathbf{X}$ in $\mathbb{R}^3$ and time t) is highly localized in a compact domain $\Omega \subset \mathbb{R}^3$, of volume $V(\Omega)$ small compared to the total volume $V(\mathcal{D})$. We assume that the fluid in $\mathcal{D}$ is homogeneous and incompressible, i.e. $\nabla \cdot \mathbf{u} = 0$, and that there are no sources or sinks of vorticity, that is $\nabla \cdot \boldsymbol{\omega} = 0$.

Numerical solutions of the real fluid equations (the Navier-Stokes equations) and real-time simulations of complex flow patterns (see, for example, the papers edited by Jiménez, 1991; Barenghi *et al.*, 1998) show that vortex lines are fundamental constituents of complex vortical flows. Recent progress in computational fluid dynamics, visualization techniques (Zabusky *et al.*, 1993; Fernandez *et al.*, 1996), and fast data processing make it possible accurate identification and detailed description of vortical structures. Formation, interaction and re-structuring of complex tangles of vortex lines can now be traced with unprecedented resolution (figure 2). Evolution and interaction of large-scale vortices (produced naturally or artificially), as well as detailed mechanisms of braiding, reconnection and linking, are all fundamental mechanisms of vortex dynamics. Geometric and topological measures provide very important information. Recent applications of geometric and topological concepts to fluid mechanics in general, and vortex dynamics in particular, have led to the development of new tools in the mathematical study of fluid flows (see the papers edited by Moffatt & Tsinober, 1990 and Moffatt *et al.*, 1992; see also Ricca & Berger, 1996). A combination of differential geometric techniques and knot theoretical tools has proved to be particularly useful (Ricca, 1998a).

In the context of the Euler equations (inviscid limit of the Navier-Stokes equations), where there is no dissipation, vortex lines are material lines frozen in the
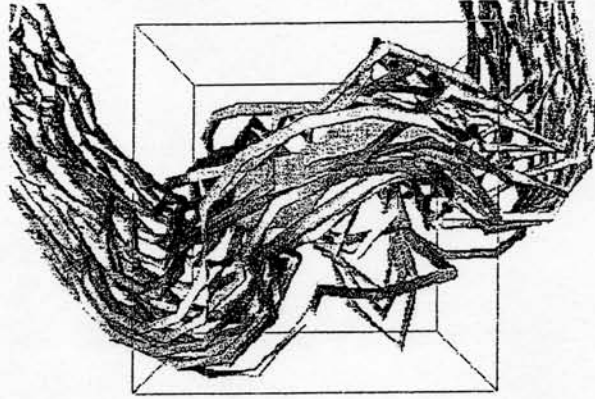
Figure 2: Close-up view of interaction and reconnection of vortex lines visualized by advanced visiometric techniques of computational fluid dynamics (from Fernandez *et al.*, 1996).

fluid (consequence of Hemholtz's theorem). Moreover vortex strength (intensity) and all topological properties are conserved (consequence of the Cauchy solutions to the Euler equations, see Saffman, 1992). Reconnections and consequential changes in vortex topology, determined by the action of dissipative effects at a microscopic physical scale, cannot take place in ideal fluids. Despite these limitations, study of ideal evolution allows a detailed understanding of the role played by geometric and topological quantities and provide us with important tools for measuring structural complexity of real vortex tangles. It is in this context that we want to present and discuss the concepts below.

2 Tropicity and linking of particle trajectories, streamlines and vortex lines

Fluid motion is induced by a smooth velocity field $\mathbf{u} = \mathbf{u}(\mathbf{X}, t)$ in $\mathcal{D}$, which satisfies the solenoidal condition $\nabla \cdot \mathbf{u} = 0$ in $\mathcal{D}$ and the condition to be at rest ($\mathbf{u} = 0$) at infinity (or on $\partial \mathcal{D}$). As time passes, fluid particles move from one position to another: if $\mathbf{a} = \mathbf{X}(\mathbf{a}, 0)$ denotes the initial position of a fluid particle at time $t = 0$, then we can define a flow map φ associated with $\mathbf{u}$, so that at each instant t a particle at $\mathbf{a}$ is sent to the final position $\mathbf{X}(\mathbf{a}, t)$ by the mapping

$$\varphi : \mathbf{a} \rightarrow \mathbf{X}, \qquad \forall t \in I , \qquad (1)$$

where I denotes some finite time interval. A *particle trajectory* $\chi_{\mathbf{a}}$ is the collection of all particle positions from $\mathbf{a}$ to $\mathbf{X}$, and is labeled by the initial position from
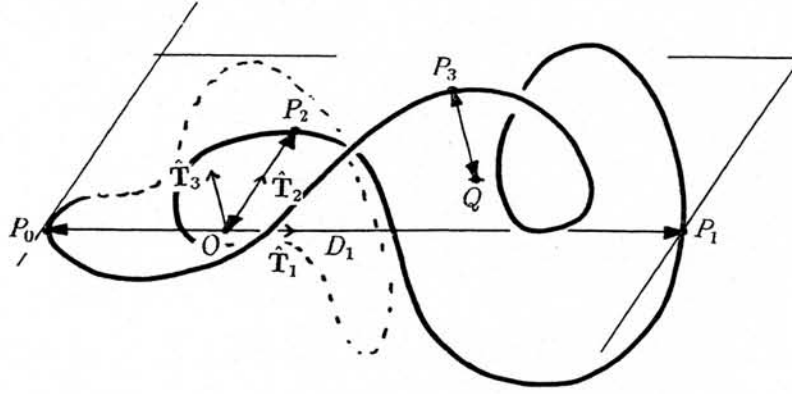
Figure 3: Directional tropic vectors of a curve in $\mathbb{R}^3$.

which it originates. Particle trajectories are the result of a time integration of positions, whereas material lines (such as streamlines or vortex lines) are instantaneous snapshots of vector field lines. In particular, at time t a *streamline* is a space curve $\Upsilon_t(s) = (x(s), y(s), z(s))$, whose directional tangent coincides with the velocity field $\mathbf{u} = (u_x, u_y, u_z)$ at each point of $\Upsilon_t(s)$, i.e.

$$\frac{dx/ds}{u_x} = \frac{dy/ds}{u_y} = \frac{dz/ds}{u_z} \,. \tag{2}$$

Similarly, a *vortex line* $\Gamma_t(s) = (x(s), y(s), z(s))$ is the embedding of the vorticity $\boldsymbol{\omega} = (\omega_x, \omega_y, \omega_z)$ onto the tangent field of $\Gamma_t(s)$, i.e.

$$\frac{dx/ds}{\omega_x} = \frac{dy/ds}{\omega_y} = \frac{dz/ds}{\omega_z} \,. \tag{3}$$

For steady flows, whose evolution is governed by autonomous velocity fields, particle trajectories and streamlines coincide.

Structural complexity of particle trajectories and material lines can be characterized according to their spatial distribution and degree of linking. The following concepts are of general applicability, regardless if referred to particle trajectories or material lines. To fix ideas let us consider a generic tangle[1] $\mathcal{T}$ of n vortex lines Γ_n, i.e. $\mathcal{T} = \bigcup_n \Gamma_n$. Let us introduce the concept of 'directional tropic vector' and 'tropic measure' to characterize the degree of tubeness, sheetness and bulkiness of $\mathcal{T}$. Take a vortex line Γ and two points P_i and P_j on Γ. The maximal extension of Γ in $\mathcal{D}$ (see figure 3) is given by

$$D_1 = \max \mathrm{d}(P_i, P_j) \equiv \overline{P_0 P_1} = \sqrt{X^2 + Y^2 + Z^2} \,, \tag{4}$$

---

[1]In this paper we do not use the word 'tangle' in a strict topological sense.

where $P_0 = (x_0, y_0, z_0)$, $P_1 = (x_1, y_1, z_1)$ and

$$X = x_1 - x_0 , \quad Y = y_1 - y_0 , \quad Z = z_1 - z_0 . \tag{5}$$

The unit vector $\hat{\mathbf{T}}_1 = (P_1 - P_0)/D_1$ given by the director cosines X/D_1, Y/D_1, Z/D_1 provides the principal directional axis of Γ in $\mathcal{D}$, and we call it *first directional tropic vector*. Let us consider the width of Γ in $\mathcal{D}$. Take the maximal distance of another point P_i on Γ (not aligned with P_0 and P_1) from the line $l(P_0, P_1)$: the width of Γ is given by

$$D_2 = \max \mathrm{d}(P_i, l(P_0, P_1)) \equiv \overline{P_2 O} , \tag{6}$$

where $O \in l(P_0, P_1)$ (O being not necessarily a point on Γ) is the orthogonal projection of P_2 on $\overline{P_0 P_1}$. As above, we can define the *second directional tropic vector* as the unit vector $\hat{\mathbf{T}}_2 = (P_2 - O)/D_2$, which gives direction and orientation of the second principal directional axis of Γ in $\mathcal{D}$. Finally, take the plane $\pi = \pi(P_0, P_1, P_2)$ and consider the maximal distance from π of a fourth point P_i on Γ, but off the plane π. A measure of the three-dimensionality of the spatial distribution of Γ in $\mathcal{D}$ is given by

$$D_3 = \max \mathrm{d}(P_i, \pi(P_0, P_1, P_2)) \equiv \overline{P_3 Q} , \tag{7}$$

along the direction of $\hat{\mathbf{T}}_3 = \hat{\mathbf{T}}_1 \times \hat{\mathbf{T}}_2$ (*third directional tropic vector*).

Now let us consider the tangle $\mathcal{T} = \bigcup_n \Gamma_n$. The above concepts of tropicity are extended to $\mathcal{T}$, where $P_i \in \mathcal{T}$ and D_i ($i = 1, 2, 3$) denotes the maximal size of $\mathcal{T}$ along the i-th principal axis. Tropic measures are used to identify a particular shape of the flow structure. The tangle configuration can be characterized by one of the following tropic quantities:

- if $D_3 = O(D_2)$ and $D_2 \ll D_1$, then we have *tubeness* $\overset{\mathrm{def}}{=} \Lambda_1 \equiv \dfrac{D_1}{D_2}$;

- if $D_3 \ll D_2$ and $D_2 = O(D_1)$, then we have *sheetness* $\overset{\mathrm{def}}{=} \Lambda_2 \equiv \dfrac{D_2^2}{D_3^2}$;

- if $D_3 = O(D_2)$ and $D_2 = O(D_1)$, then we have *bulkiness* $\overset{\mathrm{def}}{=} \Lambda_3 \equiv \dfrac{D_1 D_2 D_3}{D_3^3}$.

Other geometric measures can be employed to quantify alignment, rotation and stretching of particle trajectories and material lines, and for a discussion of these quantities we refer to the paper of Tabor (1992).

Directional tropic axes find an interesting application in the characterization of the topological entanglement of $\mathcal{T}$. A fundamental measure is given by the asymptotic linking number. The concept of linking number plays an important role in fluid dynamics (see the review article of Arnold & Khesin, 1998). For a tangle of particle trajectories (and material lines) we can define the asymptotic linking number as follows. Consider two particle trajectories $\chi_\mathbf{a}$ and $\chi_\mathbf{b}$, with $\mathbf{a} \neq \mathbf{b}$. After some long time T these trajectories are artificially closed on themselves by 'shortest paths',
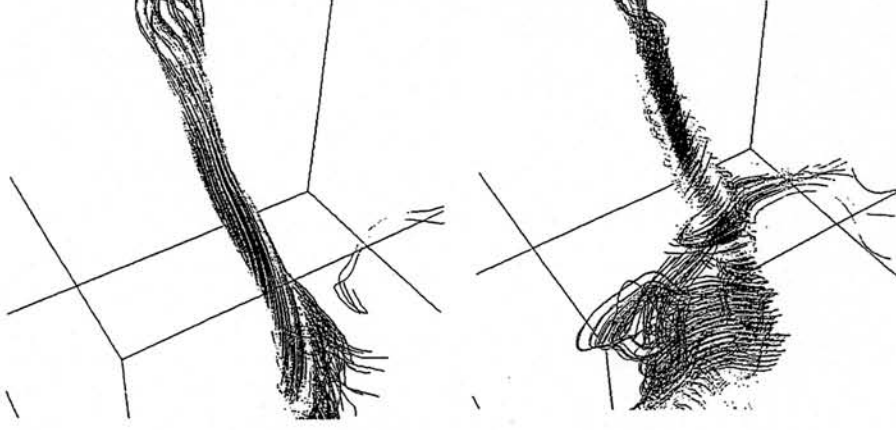
Figure 4: Close-up view of streamlines (on the left) and vortex lines (on the right) of a vortex tube in a numerical simulation of homogeneous, isotropic turbulent flow (from She *et al.*, 1990).

thereby defining two closed paths, say $\bar{\chi}_\mathbf{a}$ and $\bar{\chi}_\mathbf{b}$. The linking number $Lk(\bar{\chi}_\mathbf{a}, \bar{\chi}_\mathbf{b})$ is defined as the number of signed intersection points of $\bar{\chi}_\mathbf{a}$ with the surface bounded by $\bar{\chi}_\mathbf{b}$. The *asymptotic linking number* $\ell k(\mathbf{a}, \mathbf{b})$, associated with $\chi_\mathbf{a}$ and $\chi_\mathbf{b}$ is then defined as

$$\ell k(\mathbf{a}, \mathbf{b}) = \lim_{T \to \infty} \frac{Lk_T(\bar{\chi}_\mathbf{a}, \bar{\chi}_\mathbf{b})}{T^2} , \qquad (8)$$

where $Lk_T(\bar{\chi}_\mathbf{a}, \bar{\chi}_\mathbf{b})$ is the linking number computed for orbits integrated for time T. The limit exists for almost every pair $\mathbf{a}$, $\mathbf{b}$ and $\ell k(\mathbf{a}, \mathbf{b})$ is of L^1 class. It is useful to define also the *average linking number* $\widetilde{\ell k} = <\ell k(\mathbf{a}, \mathbf{b})>$, where $< \cdot >$ denotes average over the entire fluid domain.

A fundamental connection between topology and fluid mechanics is provided by the relationship between linking number and helicity. The average linking of any two orbits of a vector field coincides with the Hopf invariant and is indeed a measure of the helicity $\mathcal{H}$ of that field. For the vorticity field ω *kinetic helicity* is defined by

$$\mathcal{H} = \int_{\mathcal{D}} \mathbf{u} \cdot \omega \, dV , \qquad (9)$$

and is a measure of the average linking number of the tangle of vortex lines in $\mathcal{D}$.

A measure of relative linking of material lines about principal directional axes of a given flow pattern provides a useful estimate of the amount of winding localized in the flow. This measure is given by the *directional linking number* $\widetilde{\ell k}(\hat{\mathbf{T}}_i)$ defined by the degree of linking of material lines with a principal tropic axis $\vec{\lambda}_i$ (along $\hat{\mathbf{T}}_i$), i.e.

$$\widetilde{\ell k}(\hat{\mathbf{T}}_i) = <\ell k(\mathbf{a}, \hat{\mathbf{T}}_i)> , \qquad (10)$$

where

$$\ell k(\mathrm{a}, \hat{\mathrm{T}}_i) = \lim_{T \to \infty} \frac{Lk_T(\bar{\chi}_\mathrm{a}, \vec{\lambda}_i)}{T^2} \, , \tag{11}$$

and where $\vec{\lambda}_i$ is kept fixed in $\mathcal{D}$. Figure 4 shows an example of localization, where there is a high degree of tubeness and winding of streamlines and vortex lines, measured by Λ_1 and $\widetilde{\ell k}(\hat{\mathrm{T}}_1)$.

3 Measures of organised structural complexity: vortex flow in a toroidal domain

Let us first recall a fundamental result of topological fluid mechanics (see the review paper by Ricca, 1998a). For a vortex tangle $\mathcal{T}$ total helicity $\mathcal{H}$ is given by

$$H(\mathcal{T}) = \sum_i Lk_i \, \Phi_i^2 + 2 \sum_{i \neq j} Lk_{ij} \, \Phi_i \Phi_j \, , \tag{12}$$

where Lk_i is the (self-) linking number of the tube axis of the i-th vortex with respect to the framing induced by the embedding of ω in $\mathcal{D}$, and Lk_{ij} denotes the linking number of the i-th vortex with the j-th vortex. All quantities in (12) are conserved during evolution. For each vortex component we have $Lk = Wr + Tw$, and so we need a way to estimate Wr and Tw. The writhe can be measured by the sum of the signed crossings of the diagram of the vortex axis onto some projection plane, averaged over all projections, that is

$$Wr = <n_+(\nu) - n_-(\nu)> \, , \tag{13}$$

where $< \cdot >$ denotes averaging over all directions ν of projection, and $n_\pm$ denotes the number of apparent $\pm$ crossings, from the direction of projection ν. For a nearly plane curve (except small indentations to allow crossings) the writhe can be directly estimated by the sum of the signed crossings. The total twist Tw is given by the sum of the normalized total torsion

$$\frac{1}{2\pi} \int_\Gamma \tau(s) \, ds \, , \tag{14}$$

(τ torsion of the vortex axis Γ, s arc-length) and the normalized intrinsic twist of the ω-lines about Γ.

For organised vortex flows in a toroidal domain complexity can be evaluated by direct measures of topological entanglement. Let us identify Ω with a toroidal domain Π, with irrotational fluid in $\mathcal{D} - \Pi$. A vortex ring in a fluid at rest provides a good example. Let us assume that vorticity may be decomposed into a toroidal and poloidal component (along the longitudinal and meridian direction of Π, respectively), i.e. $\omega = \omega_t + \omega_p$, and that $|\omega_t| \gg |\omega_p|$. The particular form
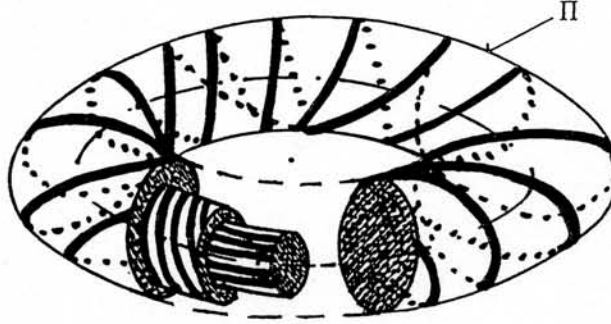
Figure 5: A collection of vortex lines uniformly coiled, knotted and linked on nested tori may provide an example of vortex ring modelling.

of the distribution, given by functional dependence of ω in Π, must satisfy a Poisson equation for vorticity, with appropriate boundary conditions on $\partial\Pi$ (Saffman, 1992). Hence, admissible distributions of vorticity must be solutions to the Poisson equation. Here we want to concentrate the attention on basic aspects of modelling, by simply assuming that the functional distribution ω (expression of the structural complexity of the flow field) is a solution of the Poisson equation. This assumption and the discussion that follows are consistent with the global theory of steady vortex rings omeomorphic to a torus (see Fraenkel & Berger, 1974). Vortex ring distributions of complex geometry and topology of the constituent vortex lines are indeed admissible as possible solutions. These include vortex lines uniformly coiled on nested tori, or in the shape of torus knots, or Hopf links on Π (figure 5).

We consider here three examples of vortex ring distributions.

Vortex coils

Take a uniform distribution of unknotted vortex coils, multi-covering a family of nested tori in $\mathcal{D}$. Complexity is given by the distribution of multi-coverings of toroidal and poloidal vortex coils, multiple foldings of the standard circle $\mathcal{U}_o$. From a geometric viewpoint we classify these coils into two categories: toroidal coils $\mathcal{U}_{m,1}$ and poloidal coils $\mathcal{U}_{1,m}$, where the first index denotes the number of times the coil wraps Π in the longitudinal direction (along the torus grand circle), and the second index denotes the number of times the coil wraps Π in the meridian direction (along the torus small circle; see figure 6).

All unknots are isotopic to one another, hence $\mathcal{U}_{m,1} \sim \mathcal{U}_{1,m} \sim \mathcal{U}_o$, and each coil contributes to the complexity of the system through individual contribution to the degree of linking Lk of the vortex ring. Here Lk denotes the limiting form of the Gauss linking number (self-linking) and is a measure of the linking of each coil with the torus axis. Since Lk is the sum of writhe Wr and total twist Tw, both decidedly
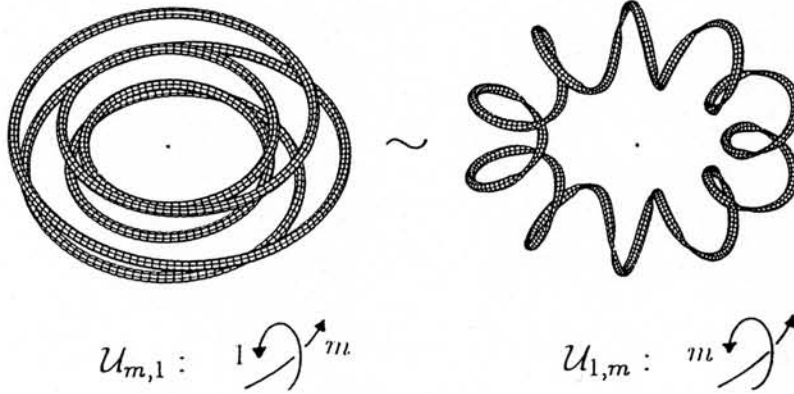
Figure 6: An example of toroidal coil $\mathcal{U}_{m,1}$ (on the left) and poloidal coil $\mathcal{U}_{1,m}$ (on the right). These coils wrap a mathematical torus Π (not visible in the figure) m times in the longitudinal (or meridian) direction and only once in the meridian (or longitudinal) direction.

non-zero, we have non-zero linking in the physical system. Hence, $Lk = m$ and the total helicity $\mathcal{H}$ (Moffatt & Ricca, 1992) amounts to

$$\mathcal{H} = \int_{\mathcal{D}} \mathbf{u} \cdot \boldsymbol{\omega}\, dV = (Wr + Tw)\, \Phi^2 = Lk\, \Phi^2 = m\, \Phi^2 \,, \tag{15}$$

where Φ is the total strength of the vortex ring. In this case m is an obvious measure of structural complexity.

Vortex knots

Vortex lines in the shape of torus knots can be taken as another example of elementary constituents of organised structural complexity. Torus knots $\mathcal{K}_{p,q}$ are closed curves wrapped around Π $p > 1$ times in the longitudinal direction, and $q > 1$ times in the meridian direction (p, q relatively prime integers; figure 7). Note that the two knots obtained by exchanging p and q (for given p and q) are topologically equivalent, i.e. $\mathcal{T}_{p,q} \sim \mathcal{T}_{q,p}$. When $p = 1$ (or $q = 1$) the curve is *not* knotted and reduces to the coil $\mathcal{U}_{1,m}$ (or $\mathcal{U}_{m,1}$). Winding number $w = q/p$ and self-linking number $Lk = pq$ provide a measure of topological complexity of the system.

Studies on vortex knots received new impetus recently, with the work of Kida (1981), Keener (1990) and Ricca (1993), who showed that vortex torus knots $\mathcal{T}_{p,q}$ that move under the so-called Localized Induction Approximation equation (LIA for short) are steady solutions of ideal fluid dynamics. LIA is however a cut-off of the Biot-Savart equation that governs the motion under the Euler equations. Numerical investigations based on the linearized equations have shown (Ricca *et al.*, 1999) that the motion consists of a simultaneous rotation and translation of the vortex filament about the symmetry axis. Aspects of stability profoundly influence the dynamics.

$$\mathcal{T}_{2,3}: \qquad q = 3 \quad p = 2 \qquad\qquad \mathcal{T}_{3,2}: \qquad q = 2 \quad p = 3$$
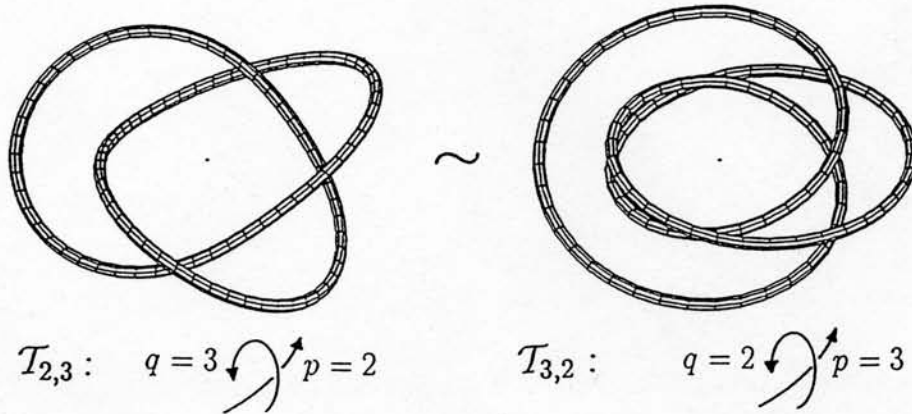
Figure 7: The standard trefoil knot $\mathcal{T}_{2,3}$ (on the left) and the isotope form $\mathcal{T}_{3,2}$ (on the right). The two knots have different geometry but are topologically equivalent.

The motion of the vortex system is studied when small-amplitude perturbations are superimposed on a steady state. If the amplitude of the perturbation decays with time, then the system is said to be stable, if it grows, then we have instability. Torus knots with winding number $w > 1$ are found to be LIA-stable, whereas the vortex knots are unstable if $w < 1$, in agreement with the stability analysis of the LIA theory (Ricca, 1993). The stable knot types tested can travel a considerable distance (compared to the maximal vortex size) in the fluid domain, without any appreciable change in shape and regardless of their complexity. Unstable knots unfold very rapidly and break down through reconnections. It is interesting to note also that poloidal and toroidal coils of the type discussed earlier are found to follow the same stability criterium: poloidal coils $\mathcal{U}_{1,m}$ are found to be LIA-stable, whereas toroidal coils $\mathcal{U}_{m,1}$ are LIA-unstable. The most interesting results, however, come from the investigation of the vortex evolution governed by the full Biot-Savart equation (no approximations involved). Torus coil and knot types are found to evolve stably, without visible change of shape, regardless of the value of their winding number, $w < 1$ or $w > 1$. This behaviour appears to be generic and independent of the complexity of the coil or knot type tested. The stabilizing action of distant parts of the vortex system, absent in the local analysis of LIA, indicates that the effects due to distant vortex elements considerably influence the long-term behaviour of the whole system.

Vortex links

Vortex lines could be linked on nested tori by Hopf links $\mathcal{L}_n^k$, where n denotes the number of components and k the degree of linking of each link type. For link systems with linking number zero (such as Borromean rings) k may be then a generalized, high-order linking number (Berger, 1990). In this case a vortex ring system is obtained by embedding n-component vortex links onto nested tori (see figure 8). In
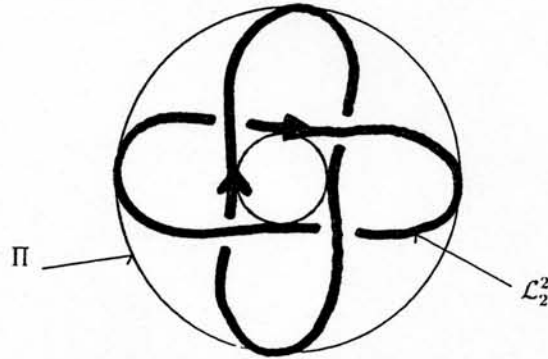
Figure 8: Example of a two-component vortex link on a mathematical torus Π: here $n = 2$ and $k = 2$.

this case a measure of complexity is given by nk.

Although studies of ideal vortex links date back to J.J. Thomson (1883; see also Ricca 1998b), no further progress has been done since. The classical results of J.J. Thomson regard motion and stability of vortex links of the type $\mathcal{L}_n^k$. These vortex link systems were found to be steady configurations, moving in the fluid without change of shape as rigid bodies. Their motion is the sum of rotation around the central axis of the torus and translation along this axis. Hence, the resulting dynamics is given by a screw motion of the whole system in $\mathcal{D}$ (as in the case of the torus knots above). Another interesting result regards stability. For n vortices $\mathcal{L}_n^k$ Thomson finds that the system is stable if $n \leq 6$, determining the period of vibration as a function of k, a result that provides an early and remarkable example of relationship between vortex dynamics and topology.

4 Geometric and topological measures for thin cored vortex filaments

Since thin cored vortex filaments are highly localized objects, their visualization and characterization is comparatively much easier than that of complex vortical flows. By identifying thin cored vortex filaments, of small circular cross section of radius σ, with their centreline Γ we can find estimates of the writhing number. An estimate based on the LIA theory (Ricca, 1995) gives

$$Wr(\Gamma) \sim \int_\Gamma (L^2 c^2 - 1)\tau \, ds \, , \tag{16}$$

where L is the total length of the vortex axis Γ, of curvature c and torsion τ. From the previous equation and the definition of self-linking number $Lk(\Gamma)$ of Γ, we have

$$Lk(\Gamma) \sim L^2 \int_\Gamma c^2 \tau \, ds \ . \tag{17}$$

Useful relations between global geometric measures and topological information are given by Milnor. A way to estimate whether Γ is knotted or not is provided by the following inequality for the total curvature of Γ (Milnor, 1950): if

$$\int_\Gamma c \, ds \geq 2\pi\beta(\Gamma) \ , \tag{18}$$

where $\beta(\Gamma)$ is the bridge index of Γ (topological invariant), then Γ is a knot. For the unknot $\mathcal{U}_o$ we have $\beta(\mathcal{U}_o) = 1$. Clearly, if

$$\int c(s) \, ds < 4\pi\beta(\Gamma) \ , \tag{19}$$

then Γ is unknotted. Moreover, the following inequalities hold true (Milnor, 1953):

$$2\pi \leq \int_\Gamma c \, ds \leq \int_\Gamma (c^2 + \tau^2)^{1/2} \, ds \leq \int_\Gamma c \, ds + \int_\Gamma |\tau| \, ds \ , \tag{20}$$

and by applying a Milnor result (1953) to our definitions of tropicity, we have

$$\int_\Gamma c \, ds + \int_\Gamma |\tau| \, ds \geq 2\pi Lk(\Gamma, \vec{\lambda_i}) \ , \tag{21}$$

where $Lk(\Gamma, \vec{\lambda_i})$ is the linking number of Γ with a directional tropic axis.

By considering the directional projection diagram of Γ, we have various estimates of the writhing number. The following results hold true:

1. (Cantarella, De Turck & Gluck, 1998):

$$|Wr(\Gamma)| \leq \frac{1}{4}\left(\frac{L}{\sigma}\right)^{4/3} \ . \tag{22}$$

Remark: if $R = 1/c$ is the local radius of curvature of Γ, then $\dfrac{L}{\sigma} > \dfrac{R}{\sigma} \gg 1$ and bounds on the writhe have no practical interest.

2. (Fuller, 1972): Let Γ_0 be a reference curve and $t_0(\xi)$ and $t(\xi)$ ($a \leq \xi \leq b$) be the tangents to Γ_0 and Γ, respectively. Then

$$|\sin \pi \left(Wr(\Gamma_0) - Wr(\Gamma)\right)| \leq 2 \int_a^b \left(\frac{3}{4(b-a)} + \left|\frac{dt_0}{d\xi}\right| + \left|\frac{dt}{d\xi}\right|\right) |t_0 - t| \, d\xi \ . \tag{23}$$

3. (Aldinger, Klapper & Tabor, 1998): Let π be an oriented plane of unit normal ν such that ν is never parallel to the tangent $\mathbf{t}$ to Γ, and Γ_0 be the ν-projection of Γ onto π (hence Γ_0 is a planar curve on π) of arc-length s_0, curvature c_0 and total length L_0. Then

$$|Wr(\Gamma) - Wr(\Gamma_0)| \le \frac{|c_0|}{2\pi} L_0 \left(1 - \frac{1}{2}\left(\frac{L_0}{L}\right)^3\right) , \qquad (24)$$

and

$$|Wr(\Gamma) - Wr(\Gamma_0)| \le \frac{1}{2\pi}\left(1 - \left(\frac{L_0}{L}\right)^2\right)^{1/2}\left(L_0 \int_{\Gamma_0} c_0^2 \, ds_0\right)^{1/2} . \qquad (25)$$

Remark: with the exception of L, obtained by direct estimates, the other quantities refer to the geometry of the planar curve Γ_0 (these quantities can be easily obtained as a by-product of the numerical code).

Another measure of topological complexity is given by the *asymptotic crossing number* $ac(\Gamma)$ introduced by Freedman & He (1991). By considering the projected diagram of Γ onto the plane of normal ν, we have

$$ac(\Gamma) = \frac{1}{4\pi} \int_\Gamma \int_\Gamma \frac{|(\mathbf{X}(s) - \mathbf{X}(s^*)) \cdot d\mathbf{X}(s) \wedge d\mathbf{X}(s^*)|}{|\mathbf{X}(s) - \mathbf{X}(s^*)|^3} = \, <n_+(\nu) + n_-(\nu)> , \quad (26)$$

where s and s^* label two different points on Γ. As for the estimate of the writhe (see previous section) $n_\pm$ denotes the number of apparent $\pm$ crossings, from the direction of projection ν, and $< \cdot >$ denotes average over all directions ν of projection. We emphasize that whereas the writhe gives a purely geometric information of the complexity of the vortex pattern, Freedman & He claim that the asymptotic crossing number provides a topological measure of the entanglement of Γ. Through application of the asymptotic crossing number, they found lower bounds for minimum energy levels of magnetic knots. Similar applications in vortex dynamics might find interesting results for energy estimates associated with changes in vortex topology due to reconnection.

5 Measures of topological entanglement of open vortex structures based on reference fields

Measures of topological entanglement of open vortex structures (figure 9) are particularly useful for numerical diagnostics and can be based on reference test fields. Relative measures of topological complexity do not provide invariant quantities, but give indications of local entanglement of the flow field. To illustrate these concepts, we follow Polifke and Levich (1991). Let us decompose the fluid domain D into two simply connected regions $D = D^\circ \bigcup D^\sharp$. If D is unbounded, we assume that all
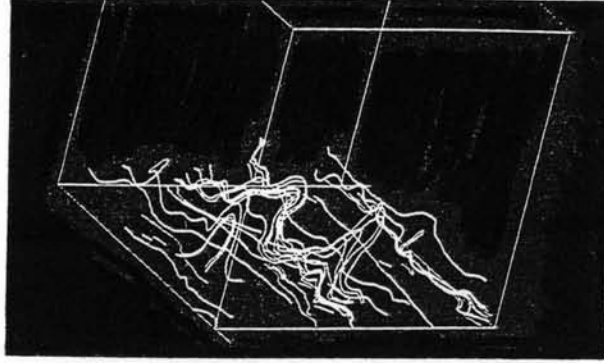
374

Figure 9: Hairpin vortex lines visualized in a numerical simulation of a boundary layer of a fluid flowing against a wall (from Lesieur (Ed.), 1991).

surface integrals vanish at infinity. Consider two fields ω^1 and ω^2, where $\omega^1 \equiv \omega$ is the given vorticity field and ω^2 is a reference vorticity field such that $\omega^2 \equiv \omega^1$ in D°. The corresponding velocity fields $\mathbf{u}^i$ are defined by $\nabla \times \mathbf{u}^i = \omega^i$ $(i = 1, 2)$. All fields are assumed to be solenoidal and smooth in D, with their normal components continuous across the boundary $\partial D^\sharp$. Berger and Field (1984) have shown that the helicity difference $\Delta \mathcal{H} = \mathcal{H}^1 - \mathcal{H}^2$ of total helicities $\mathcal{H}^i$, given by

$$\Delta \mathcal{H} = \int_D \mathbf{u}^1 \cdot \omega^1 \, dV - \int_D \mathbf{u}^2 \cdot \omega^2 \, dV \ , \tag{27}$$

is gauge invariant and depends only on the vorticity fields inside $D^\sharp$. It can be shown that

$$\Delta \mathcal{H} = \int_{D^\sharp} \nabla \xi \cdot (\omega^1 + \omega^2) \, dV - \int_{\partial D^\sharp} \xi (\omega^1 + \omega^2) \cdot \nu \, dA \ , \tag{28}$$

where $\nabla \xi = \mathbf{u}^1 - \mathbf{u}^2$, and ν is the unit normal to the surface area A of $\partial D^\sharp$. Polifke and Levich suggest that the most suitable reference field should be a potential field given by $\omega^2 = \nabla \phi$, where ϕ is a harmonic function ($\nabla^2 \phi = 0$) determined uniquely by the Neumann boundary conditions

$$\nabla \phi \cdot \nu|_{\partial D^\sharp} = \omega \cdot \nu|_{\partial D^\sharp} \ . \tag{29}$$

An alternative measure is the relative helicity $\mathcal{H}_R$ given by

$$\mathcal{H}_R \equiv \int_{D^\sharp} \mathbf{u}^1 \cdot (\omega^1 - \omega^2) \, dV \ , \tag{30}$$

which clearly requires less information than that needed for (28). Admittedly, the physical and topological interpretation of $\mathcal{H}_R$ is not so clear. Its relation with $\Delta \mathcal{H}$ is given by

$$\Delta \mathcal{H} = \mathcal{H}_R + \int_{D^\sharp} \mathbf{u}^2 \cdot (\omega^1 - \omega^2) \, dV \ , \tag{31}$$

Figure 10: A fluid structure $\mathcal{T}$ evolves under a flow map φ from the initial configuration 1 ($\mathcal{T}_1 = \varphi_1(\mathcal{T})$) to the final configuration 4 ($\mathcal{T}_4 = \varphi_4(\mathcal{T})$). Only the evolution between 2 and 3 is governed by a signature-preserving flow φ_s; hence $\mathcal{T}_2 \approx \mathcal{T}_3$, but $\mathcal{T}_1 \not\approx \mathcal{T}_4$ (i.e. $\mathcal{T}_1$ and $\mathcal{T}_4$ have different geometric signature).

where the integral term in the r.h.s of (31) is generally non-zero. However, Polifke & Levich argue that since $\nabla^2 \mathbf{u}^2 = 0$ in $D^\sharp$, the integral term above should be negligible for most field configurations, implying that $\mathcal{H}_R$ would actually provide reliable relative measures of entanglement. A number of test cases were studied by these authors to support their case.

6 Dynamical measures of structural complexity

Vortex structures may evolve by preserving geometric and topological aspects of their shape, while allowing large-amplitude deformations. Even in the presence of dissipation, we have cases where geometric features are preserved for a relatively long time compared to the typical viscous dissipation time. It is therefore necessary to extend classical concepts of dynamical stability to describe a much richer family of dynamics. Another important issue in the study of complex flow systems is 'robustness', that may characterize certain fluid evolutions, where fluid properties (such as helicity) tend to resist from decaying under dissipation. To make progress in this direction we need to introduce new concepts based on dynamical measures of structural complexity. These concepts are also useful to develop a measure theory that is able to classify structured flow patterns dynamically. Let us introduce the following:

Definition: φ_s is a *(geometric) signature-preserving flow* if it admits finite, large-amplitude deformations (diffeomorphisms) that make the final configuration recognizable in terms of the initial pattern.

Let us denote by $\mathcal{T}_t = \varphi_t(\mathcal{T})$ the instantaneous mapping of $\mathcal{T}$ by φ. If a structure $\mathcal{T}_t$ evolves under φ_s for some time $t \in I$, then we write $\mathcal{T}_{t_1} \approx \mathcal{T}_{t_2}$ (where t_1 and t_2 take values in I) to denote conservation of geometric signature (figure 10). Another important issue is vortex coherency, that can be defined as follows:

Definition: A vortex structure is said to be *coherent* if there is a spatial/temporal statistical correlation over the mean values (or higher-order moments) of the dynamical characteristics taken over a length-scale of the order of the fluid domain and a time-scale of the order of the typical evolution time of the phenomenon.

Dynamics that preserve geometric features (such as tropicity, mean curvature, writhing number, twist, etc.) and topology (knot and link type, linking number, etc.), while allowing large-amplitude deformations, have not been studied so far and there is therefore a lack of rigorous definition and analysis. Upper bounds on tropic measures, alignment and Lyapunov exponents, global and local curvatures, etc. must be used to specify the diffeomorphisms that are signature preserving from the general flow maps. Here we propose a new definition of dynamical stability in relation to these specific evolutions. By taking into account large-amplitude perturbations we can extend the usual concept of Lyapunov stability to include the dynamics governed by geometric signature-preserving flows. The corresponding motion is characterized by finite, large-amplitude, (Lyapunov) stable evolutions that conserve geometric coherency and signature for some (finite) time of physical interest. Hence, we can talk of vortex structures evolving under "stable" dynamics according to the following:

Definition: A vortex structure is said to be *(Lyapunov) stable* if it evolves under signature-preserving flows that conserve topology, geometric signature and vortex coherency.

Stable structures are therefore those able to evolve over a considerable distance (much larger than their typical length-scale), while preserving geometric signature. On the other hand, if they unfold and break-up in a short time (compared with the typical time-scale of the phenomenon), we say that they are (Lyapunov) unstable. The classification and study of flow patterns that show geometric and topological complexity, while maintaining features of (Lyapunov) stability, represent an important aspect of future research.

7 Conclusions

Self-organization of vortical tangles into coherent regions of long-lived structural complex flows seems to be a generic feature of turbulent flows. A detailed analysis of these flows requires the use of a combination of geometric and topological techniques in order to classify and measure structural complexity. In this paper we have discussed applications of various concepts that will help to develop a measure theory for complexity. In particular we have shown how classical geometric quantities (such as global measures of curvature, writhing number and relative linking estimates), topological quantities (such as link and knot type, linking number, asymptotic crossing number) and new concepts based on the degree of 'tropicity' of a flow structure (to characterize tubeness, sheetness and bulkiness of vortex flows)

can find useful applications in fluid dynamics. We have introduced the concept of directional tropicity to evaluate relative linking and estimate the degree of knottedness of a vortex pattern and we have extended the classical concept of stability to include those dynamics that preserve geometric signature during evolution. The development of a measure theory to study structural complexity finds useful applications in many physical contexts such as in polymer physics (see, for example, Kantor & Hassold, 1988; Agnes & Rasetti, 1994) and in chemical physics (see, for example, Winfree, 1994), where structured patterns are present. The concepts discussed in this paper, integrated with complementary measures of complexity developed for dynamical systems (Ghrist et al., 1997), random systems (Millett & Sumners (Ed.), 1994; Kholodenko & Rolfsen, 1996), stochastic flows and entropic systems (Badii & Politi, 1997), will be a very useful tool for carrying out efficient computational diagnostics of complex flow patterns.

Acknowledgments

References

AGNES, C. & RASETTI, M. 1994 Piecewise-linear-category approach to entanglement. *Nuovo Cimento* 3D, 121–136.

ALDINGER, J., KLAPPER, I. & TABOR, M. 1998 Formulae for the calculation and estimation of writhe. *To appear*.

ARNOLD, V.I & KHESIN, B.A. 1998 *Topological Methods in Hydrodynamics*. Applied Mathematical Sciences Series 125, Springer.

BADII, R. & POLITI, A. 1997 *Complexity*. Cambridge Nonlinear Science Series 6, Cambridge University Press.

BARENGHI, C.F., SAMUELS, D.C., BAUER, G.H. & DONNELLY, R.J. 1998 Vortex lines in a model of turbulent flow. *Phys. Fluids* 9, 2631–2643.

BERGER, M.A. 1990 Third order link invariants. *J. Phys. A: Math. & Gen.* 23, 2787–2793.

BERGER, M.A. & FIELD, G.B. 1984 The topological properties of magnetic helicity. *J. Fluid Mech.* 147, 133–148.

CANTARELLA, J., DE TURCK, D. & GLUCK, H. 1998 Upper bounds for the writhing of knots and the helicity of vector fields. *Preprint*.

FERNANDEZ, V.M., SILVER, D. & ZABUSKY, N.J. 1996 Visiometrics of complex physical processes: diagnosing vortex-dominated flows. *Computers in Phys.* 10, 463–470.

FRAENKEL, L.E. & BERGER, M.S. 1974 A global theory of steady vortex rings in an ideal fluid. *Acta Mathematica* **132**, 13–51.

FREEDMAN, M.H. & HE, Z.-X. 1991 Divergence-free fields: energy and asymptotic crossing number. *Ann. Math.* **134**, 189–229.

FULLER, F.B. 1972 How the writhing number of a curve depends on the curve. *Rev. Roum. Math. Pures Appl.* **17**, 1329–1334.

GHRIST, R.W., HOLMES, P.J. & SULLIVAN M.C. 1997 *Knots and Links in Three-Dimensional Flows*. Lecture Notes in Mathematics **1654**. Springer.

JIMÉNEZ, J. (ED.) 1991 *The Global Geometry of Turbulence*. NATO ASI Series B: Physics **268**. Kluwer.

JIMÉNEZ, J., WRAY, A.A., SAFFMAN, P.G. & ROGALLO, R.S. 1993 The structure of intense vorticity in homogeneous isotropic turbulence. *J. Fluid Mech.* **255**, 65–90.

KANTOR, Y. & HASSOLD, G.N. 1988 Topological entanglements in the percolation problem. *Phys. Rev. Lett.* **60**, 1457–1460.

KEENER, J.P. 1990 Knotted vortex filaments in an ideal fluid. *J. Fluid Mech.* **211**, 629–651.

KHOLODENKO, A.L. & ROLFSEN, D.P. 1996 Knot complexity and related observables from path integrals for semiflexible polymers. *J. Phys. A: Math. Gen.* **29**, 5677–5691.

KIDA, S. 1981 A vortex filament moving without change of form. *J. Fluid Mech.* **112**, 397–409.

LESIEUR, M. (ED.) 1991 *Images de Mecanique des Fluides Numerique*. CNRS. Institute de Méchanique de Grenoble, Grenoble, France.

MILLETT, K.C. & SUMNERS, D.W. (ED.) 1994 *Random Knotting and Linking*. Series on Knots and Everything **7**, World Scientific, Singapore.

MILNOR, J. 1950 On the total curvature of knots. *Ann. Math.* **52**, 248–257.

MILNOR, J. 1953 On total curvatures of closed space curves. *Math. Scand.* **1**, 289–296.

MOFFATT, H.K. & RICCA, R.L. 1992 Helicity and the Călugăreanu invariant. *Proc. R. Soc. Lond.* A **439**, 411–429.

MOFFATT, H.K. & TSINOBER, A. (ED.) 1990 *Topological Fluid Mechanics*. Cambridge University Press.

MOFFATT, H.K., ZASLAVSKY, G.M., COMTE, P. & TABOR, M. (ED.) 1992 *Topological Aspects of the Dynamics of Fluids and Plasmas*. NATO ASI Series E: Applied Sciences **218**. Kluwer.

POLIFKE, W. & LEVICH, E. 1990 Entangledness of vortex lines in turbulent flows. In *Topological Fluid Mechanics* (ed. H.K. Moffatt & A. Tsinober), pp. 637–646. Cambridge University Press.

RICCA, R.L. 1993 Torus knots and polynomial invariants for a class of soliton equations. *Chaos* **3**, 83–91 [1995 Erratum. *Chaos* **5**, 346].

RICCA, R.L. 1995 Geometric and topological aspects of vortex filament dynamics

under LIA. In *Small-Scale Structures in Three-Dimensional Hydro and Magnetohydrodynamics Turbulence* (ed. M. Meneguzzi *et al.*), pp. 99–104. Lecture notes in Physics **462**. Springer.

RICCA, R.L. 1998a Applications of knot theory in fluid mechanics. In *Knot Theory* (ed. V.F.R. Jones *et al.*), pp. 321–346. Banach Center Publications, Institute of Mathematics **42**, Polish Academy of Sciences, Warsaw.

RICCA, R.L. 1998b New developments in topological fluid mechanics: from Kelvin's vortex knots to magnetic knots. In *Ideal Knots* (ed. A. Stasiak *et al.*), pp. 255–273. Series on Knots and Everything **19**, World Scientific, Singapore.

RICCA, R.L. & BERGER, M.A. 1996 Topological ideas and fluid mechanics. *Phys. Today* **49** (12), 24–30.

RICCA, R.L., SAMUELS, D.C. & BARENGHI, C.F. 1999 Evolution of vortex knots. *J. Fluid Mech.* **391**, 29–44.

SAFFMAN, P.G. 1992 *Vortex Dynamics*. Cambridge University Press.

SCHWARZ, K.W. 1988 Three dimensional vortex dynamics in superfluid helium. *Phys. Rev.* B **38**, 2398–2417.

SHE, Z.-S., JACKSON, E. & ORSZAG, S.A. 1990 Intermittent vortex structures in homogeneous isotropic turbulence. *Nature* **344**, 226–228.

TABOR, M. 1992 Stretching and alignment in general flow fields: classical trajectories from Reynolds number zero to infinity. In *Topological Aspects of the Dynamics of Fluids and Plasmas* (ed. H.K. Moffatt ıet al.), pp.83–110. NATO ASI Series E: Applied Sciences **218**. Kluwer.

THOMSON, J.J. 1883 *A Treatise on the Motion of Vortex Rings*. MacMillan & Co., London.

VINCENT, A. & MENEGUZZI, M. 1991 The spatial structure and statistical properties of homogeneous turbulence. *J. Fluid Mech.* **225**, 1–25.

WINFREE, A.T. 1994 Persistent tangles of vortex rings in generic excitable media. *Nature* **371**, 233–236.

ZABUSKY, N.J., SILVER, D. & PELZ, R. 1993 Visiometrics, juxtaposition and modeling. *Phys. Today* **46**, 24–31.